INVESTIGATION OF UPSTREAM LENGTH REQUIREMENTS FOR VENTURI TUBE INSTALLATION USING CFD

[1]A.Tukimin, [2]M.Zuber, [2]K.A.Ahmad, [2]S.Saadon

[1]Department of Mechanical and Manufacturing Engineering, Faculty of Engineering, Universiti Putra Malaysia, Jalan Upm, 43400 Serdang, Selangor, Malaysia

[2]Department of Aerospace Engineering, Faculty of Engineering, Universiti Putra Malaysia, Jalan Upm, 43400 Serdang, Selangor, Malaysia

For Correspondence; agustinnie@gmail.com, *mdzubairmanipal@gmail.com

ABSTRACT: *The installation of Venturi tubes for high accuracy flow measurement in industrial application is normally based on the available international standards and guidelines. The international standard ISO 5167-4 provides guidelines on the installation requirements for Venturi in terms of upstream straight length requirements and configurations. This guideline indicates that any installation with upstream straight length lesser than the given minimum value, will incur additional 0.5% uncertainty on the discharge coefficient of the Venturi tube. The approach indicated by the international standard is very general and conservative.*

In this work, the numerical simulation was used to investigate the impact on the discharge coefficient, Cd, for installation with upstream straight length lesser than the given minimum value by comparing the numerical simulation results and experimental data, for Venturi tubes ranging from 100 mm to 250 mm. It was found that the numerical simulation results were within +/- 0.5% uncertainty and this is in line with the guidelines by the international standard.

1. INTRODUCTION

As the differential pressure type flow meter, such as Venturi and orifice plate, becomes more applicable in the accurate flow metering applications, the understanding on its performance in various installation configurations is becoming critical in order to ensure the overall measurement accuracy requirement is met.

Earlier works of Himpe et al. on the influence of upstream bends on the discharge coefficients, Cd, of classical Venturi tubes and orifice plates indicated that the for pipe bends upstream of an orifice with undisturbed inlet sections smaller, as demanded in ISO 5167-1, it was recommended to install the pressure taps in the direction of the inner side of the bend (0^o angle position) [1].

Another works by Reader-Harris et al. focused on experimental works in the allowable steps in pipework upstream of orifice plates. The results of the works indicated that if the very first fitting is placed 10D (D is the internal pipe diameter) upstream of the orifice plate, the existing necessities of 0.3% of D are unduly restrictive and that expansion steps of up to 2% of D and contraction steps up to 6% of D can be permitted [2].

In 2003, International Standardization Organization (ISO) committee produced the revision 2003 of the ISO 5167 international standard which covers the guidelines on upstream straight requirement for differential pressure devices, such as Venturi tubes and orifice plates.

This paper presents the work on using Computational Fluid Dynamics (CFD) to investigate the impact of upstream straight length on the measurement accuracy of Venturi tubes, in accordance to ISO 5167-4 [3].

2. SCOPE OF THE WORK

Venturi tubes

The work uses the Venturi tube with sizes ranging from 100 mm to 250 mm of internal pipe diameter. The Venturi tubes' pressure rating is ASME 900 lbs, with 21° convergent angle and 15° divergent angle of the inlet and outlet cones, respectively.

Upstream straight length

The numerical simulation focuses on 10D and 3D upstream straight length installation configurations. According to ISO 5167-4, 10D upstream straight length is the minimal requirement for "zero additional uncertainty" on discharge coefficient. The 3D upstream straight length is selected as ISO 5167-4 indicates any upstream straight length between 10D and 3D gives "0.5% additional uncertainty" to the discharge coefficient, and this is the shortest upstream straight length indicated by the guideline which provides useable additional uncertainty value to be used in the measurement.

3. METHODS

The work involved setting up the models in the ANSYS DesignModeller, similar to the physical Venturi tubes used in the experimental calibration. The numerical simulation was performed on these models. The outputs of the numerical simulation, which are the velocities and differential pressures, were then used to calculate the discharge coefficient of the Venturi tubes.

The discharge coefficient, Cd, was calculated using Eq. (1):

$$Cd = 4m(1-\beta^4)^{0.5} / (\pi \varepsilon d^2) / (200000 Dp_1 \rho_1)^{0.5} \quad (1)$$

Where m is the reference gas mass flow rate (kg/s), β is the diameter ratio (-), ε is the gas expansibility (-), d is the internal throat diameter (m), ρ_1 is the upstream gas density (kg/m^3) and Dp_1 is the measure of upstream-to-throat differential pressure (bar) [4].

Experimental calibration

The National Engineering Laboratory (NEL) in the United Kingdom was used to perform the experimental calibration of the Venturi tubes. The experimental setup was based on 20D upstream straight length pipe spool, which is way beyond the minimum "zero additional uncertainty" upstream straight length as indicated by ISO 5167-4. The nitrogen gas was used as the calibration gas, with varying flow rates and velocities applied during the test.

The collected calibration data was used as the baseline reference when comparing the discharge coefficient between experiment and numerical simulation.

Table 1, 2, 3 and 4 provide the overview of the test matrix for each size of the Venturi tubes.

Table 1: Test matrix for 100 mm Venturi tube

Test Point	Pressure	Temperature	Gas Flowrate	Nitrogen density	Gas superficial velocity
(-)	(bar)	(°C)	(m^3/h)	kg/m^3	m/s
1	24.60	17.95	398	29.781	14.89
2	24.56	17.92	298	29.738	11.18
3	24.52	17.96	199	29.687	7.46
4	24.49	17.91	100	29.657	3.73

Table 2: Test matrix for 150 mm Venturi tube

Test Point	Pressure	Temperature	Gas Flowrate	Nitrogen density	Gas superficial velocity
(-)	(bar)	(°C)	(m^3/h)	kg/m^3	m/s
1	24.75	19.91	995	29.743	20.25
2	24.67	19.97	854	29.643	17.39
3	24.60	20.05	713	29.554	14.51
4	24.54	20.01	571	29.488	11.62

Table 3: Test matrix for 200 mm Venturi tube

Test Point	Pressure	Temperature	Gas Flowrate	Nitrogen density	Gas superficial velocity
(-)	(bar)	(°C)	(m^3/h)	kg/m^3	m/s
1	50.06	20.03	1559	59.031	14.70
2	49.95	20.06	1208	58.898	11.39
3	49.87	19.99	908	58.821	8.56
4	50.45	19.84	609	59.525	5.74

Table 4: Test matrix for 250 mm Venturi tube

Test Point	Pressure	Temperature	Gas Flowrate	Nitrogen density	Gas superficial velocity
(-)	(bar)	(°C)	(m^3/h)	kg/m^3	m/s
1	59.98	20	1217	70.483	7.02
2	59.95	19.9	1043	70.476	6.02
3	59.91	19.95	869	70.416	5.02
4	59.89	19.93	696	70.398	4.01

Computational setup

The model consisted of the internal section of the Venturi tube. The inflation at the internal wall of the tube was used in the meshing to gain better details of the pressure distribution near the wall, as given in Fig. 1. As part of grid independence check, the model was simulated for different mesh size from coarse to fine so as to assure that there will not be any change in the solution by further refining the mesh.
The 2-dimensional symmetry had been used for the analysis of the simulation outputs. Pressure based solver and SIMPLE pressure-velocity coupling had been used as these are applicable for wide range of flow regimes.

All the cases in the simulation were based on the turbulent flow regime, as all the test points in the physical experiment calibration were in the turbulent flow regime. The Standard K-Epsilon (SKE) turbulence model had been used in the simulation that solves for two variables, turbulent kinetic energy, K and rate of dissipation of kinetic energy, Epsilon. The SKE turbulence model was selected because of its good convergence rate and relatively low memory requirements [5].

The boundary conditions were set according to the velocities, pressures, temperatures and densities, similar to the physical Venturi tubes being used in the experimental test for each of the test points.

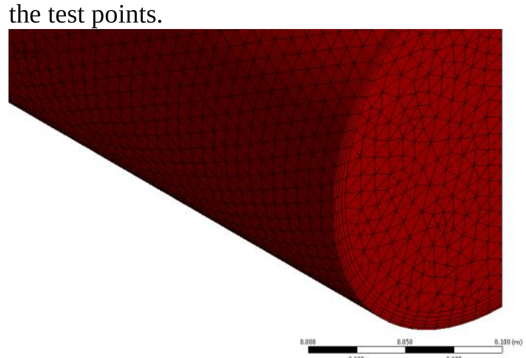

Fig. 1: Inflation layers close to the internal wall

Comparative investigation

The discharge coefficient obtained from numerical simulation for Venturi tube installed with 10D upstream straight length was first compared against the discharge coefficient obtained from experimental test. This comparison was used as the baseline reference for the next phase of the numerical simulation analysis.

The next phase of the numerical simulation focused on processing the results for Venturi tube installed with 3D upstream straight length. The discharge coefficient obtained from the simulation for shorter upstream straight length were then compared against the discharge coefficient obtained from simulation for 10D upstream straight length.

The impact on the change of internal pipe diameter, velocity and pressure were also recorded and compared.

4. RESULTS AND DISCUSSION

The numerical simulation results indicate the discharge coefficients between Venturi tube with 10D upstream straight length and Venturi tube with 3D upstream straight length are within +/-0.5% error (uncertainty), as shown in Table 15.

Contours for velocities and pressure distributions

Figures Fig. 2, 3, 4, 5, 6, 7, 8 and 9 are the velocity contours for all the configurations of the upstream straight length and Venturi tubes' sizes. Flow direction for all the contours are from left to right. Velocity values recorded from the contours below are used to calculate the volumetric flow rates. 20-colors legend has been used to ensure the different velocities can be made visible.

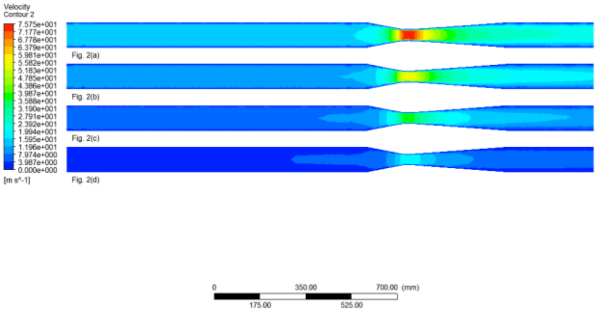

Fig. 2: Velocity contour for 100 mm Venturi tube with 10D upstream straight length

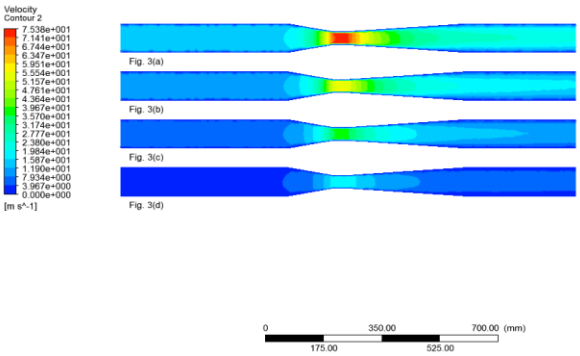

Fig. 3: Velocity contour for 100 mm Venturi tube with 3D upstream straight length

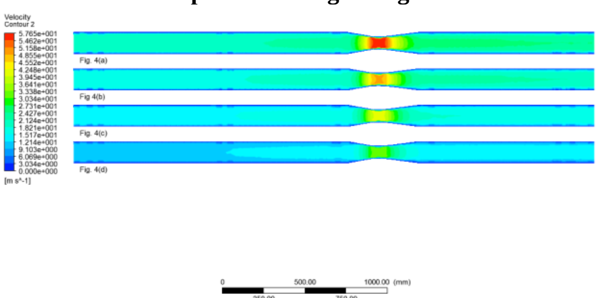

Fig. 4: Velocity contour for 150 mm Venturi tube with 10D upstream straight length

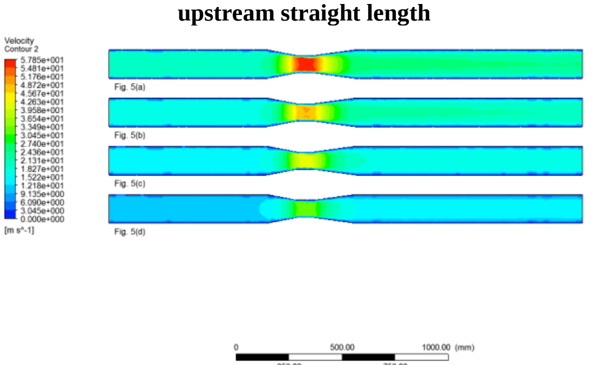

Fig. 5: Velocity contour for 150 mm Venturi tube with 3D upstream straight length

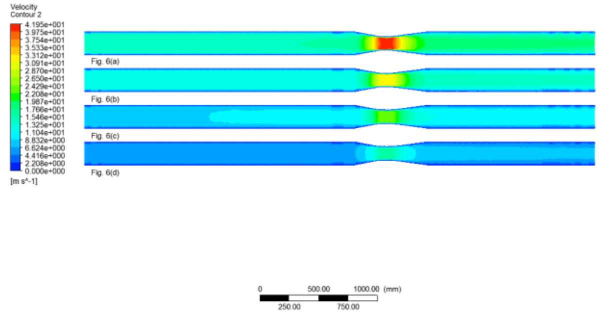

Fig. 6: Velocity contour for 200 mm Venturi tube with 10D upstream straight length

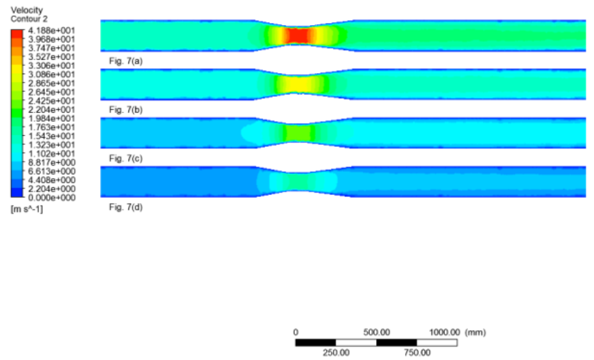

Fig. 7: Velocity contour for 200 mm Venturi tube with 3D upstream straight length

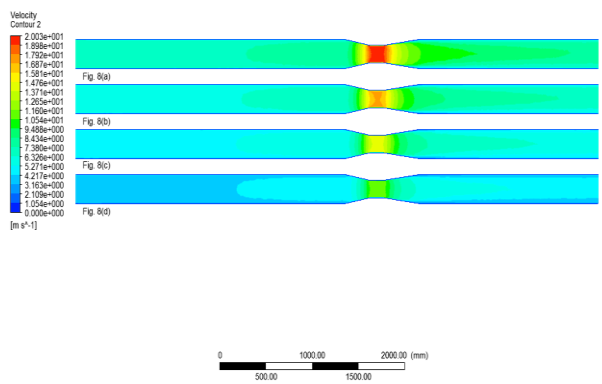

Fig. 8: Velocity contour for 250 mm Venturi tube with 10D upstream straight length

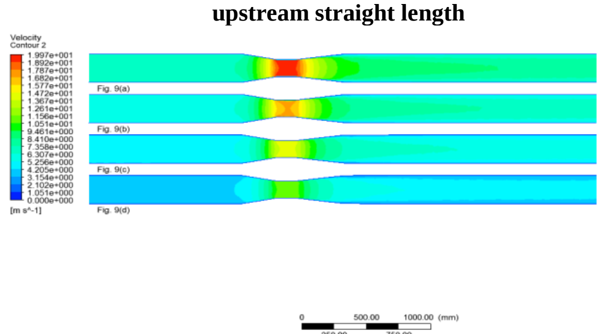

Fig. 9: Velocity contour for 250 mm Venturi tube with 3D upstream straight length

Figures Fig. 10, 11, 12, 13, 14, 15, 16 and 17 are the pressure distribution contours for all the configurations of the upstream straight length and Venturi tubes' sizes. Flow direction for all the contours are from left to right. Pressure values recorded, at the upstream of the Venturi and at its throat, from the contours below are used in the flow calculations. 20-colors legend has been used to ensure the different velocities can be made visible.

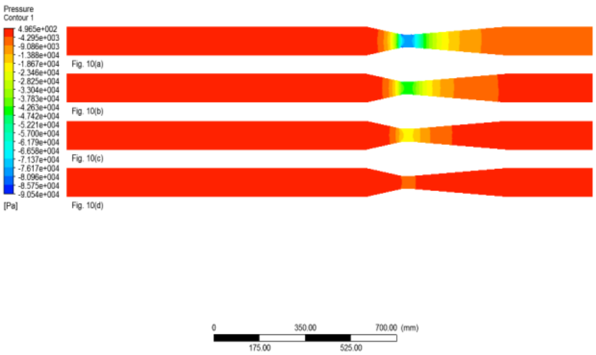

Fig. 10: Pressure distribution contour for 100 mm Venturi tube with 10D upstream straight length

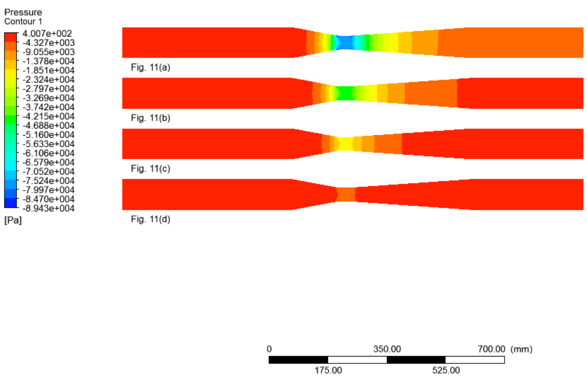

Fig. 11: Pressure distribution contour for 100 mm Venturi tube with 3D upstream straight length

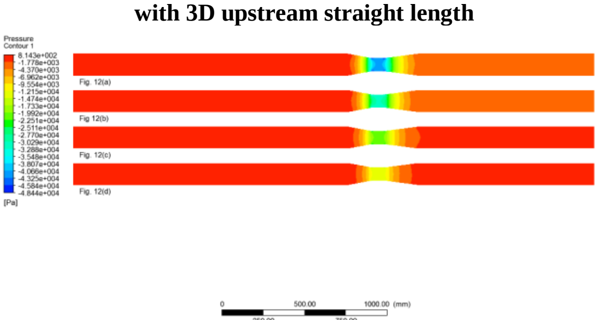

Fig. 12: Pressure distribution contour for 150 mm Venturi tube with 10D upstream straight length

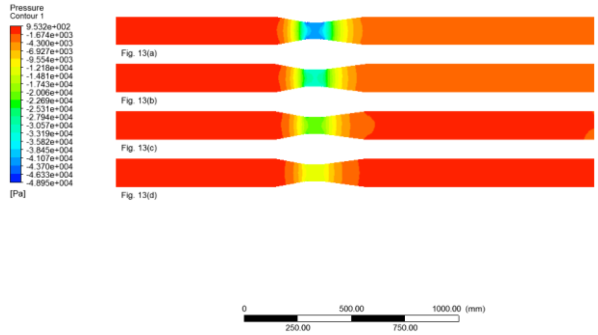

Fig. 13: Pressure distribution contour for 150 mm Venturi tube with 3D upstream straight length

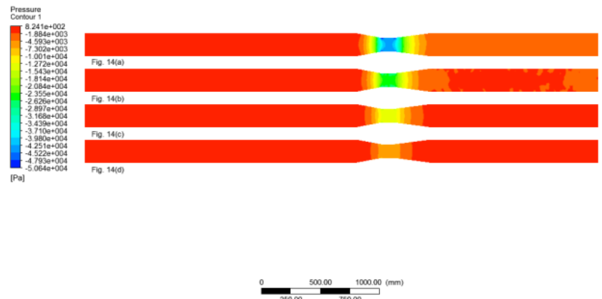

Fig. 14: Pressure distribution contour for 200 mm Venturi tube with 10D upstream straight length

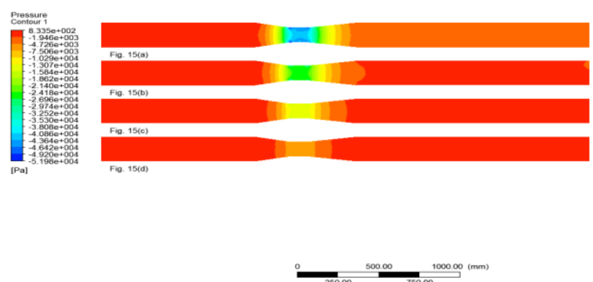

Fig. 15: Pressure distribution contour for 200 mm Venturi tube with 3D upstream straight length

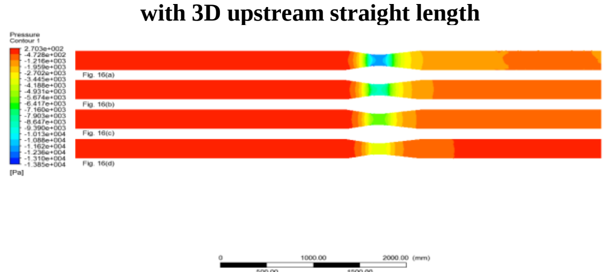

Fig. 16: Pressure distribution contour for 250 mm Venturi tube with 10D upstream straight length

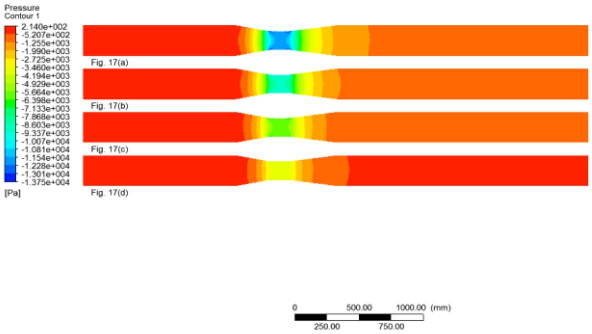

Fig. 17: Pressure distribution contour for 250 mm Venturi tube with 3D upstream straight length

Discharge coefficients from numerical simulation

Table 5, 6, 7 and 8 provide the discharge coefficients, calculated using the outputs of the numerical simulation for Venturi tubes with 10D upstream straight length. The average values of these discharge coefficients are compared against the discharge coefficient values from experimental, and this comparison is tabulated in Table 9.

For Venturi tubes' sizes 100 mm, 150 mm and 200 mm, it is clearly shown that the discharge coefficient error decreases with the increase in velocity. Viscosity and density are kept within small variances for all these cases. On the basis on these computations, it is clear that the discharge coefficient is a function of Reynolds number [6]. The change in the Venturi tubes' size does not impact the discharge coefficient error trend. For 250 mm Venturi tube, different trending shown in the discharge coefficient error is due to the close velocity cases selected for the test.

Table 5: Discharge coefficient for 100 mm Venturi with 10D upstream straight length

Test	Dp1 (From ANSYS)	Pressure	Temp.	Velocity (From ANSYS)	Mass Flowrate	Discharge Coefficient	Error (compared to experiment)
	bar	bar	(°C)	m/s	kg/hr		
1	0.78224	24.60	17.95	14.90	11846.18	1.01231	2.16%
2	0.44093	24.56	17.92	11.19	8882.71	1.00367	1.28%
3	0.19612	24.52	17.96	7.46	5917.15	0.99763	0.67%
4	0.04905	24.49	17.91	3.73	2955.80	0.99355	0.26%

Table 6: Discharge coefficient for 150 mm Venturi with 10D upstream straight length

Test	Dp1 (From ANSYS)	Pressure	Temp.	Velocity (From ANSYS)	Mass Flowrate	Discharge Coefficient	Error (compared to experiment)
	bar	bar	(°C)	m/s	kg/hr		
1	0.41548	24.75	19.91	20.35	29727.67	1.00831	0.89%
2	0.30540	24.67	19.97	17.48	25446.17	1.00557	0.61%
3	0.21204	24.60	20.05	14.58	21169.54	1.00313	0.37%
4	0.13573	24.54	20.01	11.68	16917.54	1.00112	0.17%

Table 7: Discharge coefficient for 200 mm Venturi with 10D upstream straight length

Test	Dp1 (From ANSYS)	Pressure	Temp.	Velocity (From ANSYS)	Mass Flowrate	Discharge Coefficient	Error (compared to experiment)
	bar	bar	(°C)	m/s	kg/hr		
1	0.43229	50.06	20.03	14.72	92175.69	1.00195	0.94%
2	0.25902	49.95	20.06	11.41	71261.03	0.99973	0.72%
3	0.14616	49.87	19.99	8.57	53487.94	0.99824	0.57%
4	0.06654	50.45	19.84	5.75	36298.76	0.99707	0.45%

Table 8: Discharge coefficient for 250 mm Venturi with 10D upstream straight length

Test	Dp1 (From ANSYS)	Pressure	Temp.	Velocity (From ANSYS)	Mass Flowrate	Discharge Coefficient	Error (compared to experiment)
	bar	bar	(°C)	m/s	kg/hr		
1	0.11831	59.98	20	7.03	85876.16	0.99533	-0.51%
2	0.08615	59.95	19.9	6.03	73637.45	0.99991	-0.05%
3	0.05987	59.91	19.95	5.03	61355.06	0.99961	-0.08%
4	0.03819	59.89	19.93	4.02	49000.50	0.99943	-0.10%

Table 9: Comparison between experimental and numerical simulation (10D upstream)

Venturi size	Cd from experiment	Cd from ANSYS	Error (%)
100 mm	0.99095	1.00179	1.09%
150 mm	0.99945	1.00453	0.51%
200 mm	0.99260	0.99925	0.67%
250 mm	1.00044	0.99857	-0.19%

Table 10, 11, 12 and 13 provide the discharge coefficients, calculated using the outputs of the numerical simulation for Venturi tubes with 3D upstream straight length. The average values of these discharge coefficients are compared against the discharge coefficient values from experimental, and this comparison is tabulated in Table 14.

Table 10: Discharge coefficient for 100 mm Venturi with 3D upstream straight length

Test	Dp1	Pressure	Temp.	Velocity	Mass Flowrate	Discharge Coefficient	Error (compared to experiment)
	(From ANSYS)			(From ANSYS)			
	bar	bar	(°C)	m/s	kg/hr		
1	0.78291	24.60	17.95	14.94	11880.06	1.01478	2.41%
2	0.44094	24.56	17.92	11.22	8908.28	1.00654	1.57%
3	0.19613	24.52	17.96	7.49	5935.27	1.00065	0.98%
4	0.04906	24.49	17.91	3.75	2966.05	0.99695	0.61%

Table 11: Discharge coefficient for 150 mm Venturi with 3D upstream straight length

Test	Dp1	Pressure	Temp.	Velocity	Mass Flowrate	Discharge Coefficient	Error (compared to experiment)
	(From ANSYS)			(From ANSYS)			
	bar	bar	(°C)	m/s	kg/hr		
1	0.41730	24.75	19.91	20.42	29835.34	1.00981	1.04%
2	0.30671	24.67	19.97	17.54	25542.12	1.00725	0.78%
3	0.21296	24.60	20.05	14.64	21250.98	1.00484	0.54%
4	0.13633	24.54	20.01	11.73	16984.31	1.00289	0.34%

Table 12: Discharge coefficient for 200 mm Venturi with 3D upstream straight length

Test	Dp1	Pressure	Temp.	Velocity	Mass Flowrate	Discharge Coefficient	Error (compared to experiment)
	(From ANSYS)			(From ANSYS)			
	bar	bar	(°C)	m/s	kg/hr		
1	0.43484	50.06	20.03	14.74	92303.44	1.00042	0.79%
2	0.26057	49.95	20.06	11.42	71362.24	0.99820	0.56%
3	0.14704	49.87	19.99	8.58	53565.51	0.99671	0.41%
4	0.06695	50.45	19.84	5.75	36290.10	0.99378	0.12%

Table 13: Discharge coefficient for 250 mm Venturi with 3D upstream straight length

Test	Dp1	Pressure	Temp.	Velocity	Mass Flowrate	Discharge Coefficient	Error (compared to experiment)
	(From ANSYS)			(From ANSYS)			
	bar	bar	(°C)	m/s	kg/hr		
1	0.11929	59.98	20	7.05	86133.83	0.99423	-0.62%
2	0.08776	59.95	19.9	6.05	73863.94	0.99376	-0.67%
3	0.06101	59.91	19.95	5.04	61549.62	0.99331	-0.71%
4	0.03895	59.89	19.93	4.03	49161.94	0.99284	-0.76%

Table 14: Comparison between experimental and numerical simulation (3D upstream)

Venturi size	Cd from experiment	Cd from ANSYS	Error (%)
100 mm	0.99095	1.00473	1.39%
150 mm	0.99945	1.00620	0.68%
200 mm	0.99260	0.99727	0.47%
250 mm	1.00044	0.99354	-0.69%

For Venturi tubes' sizes 100 mm, 150 mm and 200 mm with 3D upstream straight length, similar trend whereby the discharge coefficient error decreases with the increase in velocity is shown for these sizes, except for the 250 mm size.

It is clearly shown that the discharge coefficient error is larger for the Venturi tubes with 3D upstream straight length when compared with the experimental discharge coefficient. This supports the general guideline that having shorter upstream length will increase the discharge coefficient error.
Table 15 compares the discharge coefficients obtained from Venturi tube with 10D upstream straight length and Venturi tube with 3D upstream straight length numerical simulation. It is shown that the discharge coefficient errors between the two sets of data are well within +/-0.5% as expected, similar to the ISO 5167-4 guideline. However, it is also shown that these errors can be biased to positive error or negative error. Earlier in this paper, it was indicated that the size of the Venturi tube does not impact the discharge coefficient error. The discharge coefficient error trend shown in Table 15 indicates that pressure contributes to the bias in error. It is shown that low pressure (approximately 24 bar) for Venturi sizes 100 mm and 150 mm gives positive bias discharge coefficient error, and high pressure (approximately 50 bar and 60 bar) for Venturi sizes 200 mm and 250 mm gives negative bias discharge coefficient error.

Table 15: Comparison between 3D and 10D upstream of the numerical simulations

Venturi size	Cd (10D upstream)	Cd (3D upstream)	Error (%)
100 mm	1.00179	1.00473	0.29%
150 mm	1.00453	1.00620	0.17%
200 mm	0.99925	0.99727	-0.20%
250 mm	0.99857	0.99354	-0.50%

5. CONCLUSION

The numerical simulation can be used in the design for optimum solution whenever available upstream straight length is insufficient for high accuracy installation as results from this work indicate the discharge coefficients between Venturi tube with 10D upstream straight length and Venturi tube with 3D upstream straight length are within +/-0.5% error (uncertainty). Although the Venturi sizes do not impact the error in the discharge coefficient, velocity and pressure of the process tremendously affect the accuracy of the measurement.

6. ACKNOWLEDGEMENTS

Authors acknowledge the assistance from FRGS grant 5524612, as well as support from NEL.

7. REFERENCES

[1] Himpe, U., Gotte, B. and Schatz, M. Influence of upstream bends on the discharge coefficients of classical Venturi tubes and orifice plates. Flow measurement instrument 1994, Vol. 5 No. 3: 209-216 (1994).

[2] Reader-Harris, M.J., Sattary, J.A. and Spearman, E.P., 1995. Orifice plate discharge coefficient equation – further work. Flow measurement and instrumentation 6: 101-114 (1995).

[3] International Organization for Standardization, 2003. Measurement of fluid flow by means of pressure differential devices inserted in circular cross-section conduits running full, Part 4: Venturi tubes. BS EN ISO 5167-4 (2003).

[4] Fang, L. and Zhang, T., 2008. Chinese Journal of Chemical Engineering, 16: 320-324;

[5] Sowjanya, V. and Jie, C. Applied Mathematical Modelling, 34: 1458-1466 (2010).

[6] Sattary, J.A. and Reader-Harris, M.J. North Sea Flow Measurement Workshop, Paper 4.6 (1997).